



Original Article



Activation of NLRP3 Inflammasome via Drp1 Overexpression in Kupffer Cells Aggravates Ischemia-reperfusion Injury in Hepatic Steatosis

Lu Zhang^{1#}, Mingfu Wang^{2#}, Ran An¹, Jun Dai³, Shujun Liu⁴, Ming Chen^{1*}  and Haoran Ding^{1*} 

¹Department of Hepatobiliary Surgery, Affiliated Drum Tower Hospital of Nanjing University Medical School, Nanjing, Jiangsu, China; ²Surgery Department I, Zhangjiagang Traditional Chinese Medicine Hospital, Suzhou, Jiangsu, China; ³Department of Hepatobiliary Surgery, The First Affiliated Hospital of Wannan Medical College, Wuhu, Anhui, China; ⁴Department of Hepatobiliary Surgery, Nanjing Drum Tower Hospital, Clinical College of Traditional Chinese and Western Medicine, School of Pharmacy, Nanjing University of Chinese Medicine, Nanjing, Jiangsu, China

Received: 16 November 2022 | Revised: 23 February 2023 | Accepted: 16 March 2023 | Published online: 23 May 2023

Abstract

Background and Aims: Donors with fatty livers are considered to address the shortage of livers for transplantation, but those livers are particularly sensitive to ischemia-reperfusion injury (IRI), and an increased incidence of graft failure is observed. Kupffer cells account for 20–35% of liver nonparenchymal cells, and have been shown to participate in the process of IRI and inflammatory reactions of hepatic steatosis. NOD-like receptor thermal protein domain-associated protein 3 (NLRP3) is an intracellular sensor activated by Kupffer cells to promote generation and participates in IRI. Dynamics-associated protein 1 (Drp1) is one of the main proteins regulating mitochondrial division and exacerbates IRI by affecting mitochondrial dynamics. The mechanism of interaction of Kupffer cells with Drp1 and NLRP3 to aggravate IRI has not been clarified. **Methods:** A mouse model of hepatic steatosis was established by feeding the mice with a high-fat diet. *In vitro* experiments were performed using AML12 normal mouse liver cells and RAW264.7 mononuclear macrophage cells cultured in medium with palmitate and oleic acid. Western blotting and immunohistochemical (IHC) staining were used to detect the expression of NLRP3 and Drp1 in IRI in the control and high-fat diet groups. The expression of F4/80+ cells during IRI in hepatic steatosis was verified by IHC staining, and the role of NLRP3 and Drp1 in Kupffer-cell mediated IRI was investigated by targeting Drp-1 inhibition. **Results:** Drp1 and NLRP3 expression was

increased during IRI in hepatic steatosis, and the expression of Drp1 and NLRP3 were decreased after the elimination of Kupffer cells. That indicated Kupffer cells were involved in the process of IRI in hepatic steatosis through the action of Drp1 and NLRP3. After Drp1 inhibition, liver function was restored and NLRP3 expression level was reduced. **Conclusions:** Kupffer cells aggravated IRI in hepatic steatosis via NLRP3 and Drp1. Drp1 inhibitors might be useful as specific therapeutics to alleviate IRI in hepatic steatosis and may have promise in case of liver donor shortage.

Citation of this article: Zhang L, Wang M, An R, Dai J, Liu S, Chen M, et al. Activation of NLRP3 Inflammasome via Drp1 Overexpression in Kupffer Cells Aggravates Ischemia-reperfusion Injury in Hepatic Steatosis. *J Clin Transl Hepatol* 2023;11(5):1069–1078. doi: 10.14218/JCTH.2022.00109.

Introduction

Scarcity of liver donor limits liver transplantation. As marginal donors, donors with fatty liver are promising candidates to increase the number of livers for transplantation.¹ In China, the percentage of donors with fatty liver is as high as 15–40% of all liver donors. The donors with hepatic steatosis are particularly susceptible to ischemia-reperfusion injury (IRI), and the incidence of nonfunction of the grafts after transplantation is very high.² This deleterious outcome may be related to the high correlation between proinflammatory activation of innate immune and inflammatory response. Innate immune cells in the liver are mainly Kupffer cells (KCs), which are innate macrophages of the liver. They account for 80–90% of the total number of macrophages and are a considerable link of the mononuclear macrophage system.³ Activated KCs produce various mediators aggravating hepatic inflammation and dysregulation of fat metabolism.^{4,5} The progression of hepatic steatosis and underlying inflammatory reaction are closely related to the interaction between macrophages and hepatocytes. Therefore, macrophages play a crucial role in the pathophysiology of hepatic steatosis and inflammation.⁶ NOD-like receptor thermal protein domain-associated

Keywords: Drp1; Kupffer cells; NLRP3; Hepatic steatosis; Ischemia-reperfusion.

Abbreviations: CCK-8, cell counting kit-8; CLO, clodronate liposomes; Drp1, dynamics-associated protein 1; ELISA, enzyme-linked immunosorbent assay; H&E, hematoxylin and eosin; IHC, immunohistochemistry; IRI, ischemia-reperfusion injury; KCs, Kupffer cells; NAFLD, nonalcoholic fatty liver disease; NLRP3, NOD-like receptor thermal protein domain-associated protein 3; ROS, reactive oxygen species; RT-qPCR, real-time quantitative polymerase chain reaction SD, standard deviation; UCP-2, uncoupling protein-2.

*Contributed equally to this work.

Correspondence to: Ming Chen and Haoran Ding, Department of Hepatobiliary Surgery, Affiliated Drum Tower Hospital of Nanjing University Medical School, Nanjing, Jiangsu 210008, China. ORCID: <https://orcid.org/0000-0002-1627-6189> (MC) and <https://orcid.org/0000-0001-8510-4623> (HD). Tel/Fax: +86-25-83106666, E-mail: chenming@njglyy.com (MC) and dhr1118@163.com (HD)

protein 3 (NLRP3) is an intracellular sensor.⁷ NLRP3 inflammasomes are produced by pathogen stimulation, immune signals, and inflammatory stimuli.⁸ Wang *et al.*⁹ reported that itaconic acid can inhibit the activity of NF- κ B pathway and affect the downstream expression of NLRP3, thereby alleviating liver dysfunction and inflammation responses. IRI involves inflammation, apoptosis, and other pathological processes associated with mitochondrial dysfunction.

Mitochondrial dynamics regulate the structure and function of mitochondria, which is represented by the fusion and division of mitochondria.¹⁰ Dynamics-associated protein 1 (Drp1) regulates mitochondrial division.¹¹ Qasim *et al.*¹² reported that in intestinal ischemia-reperfusion, the expression of p-Drp1 and Ser637 decreased and translocation of Drp1 to mitochondrial outer membrane was inhibited, thus inhibiting mitochondrial division to improve cell damage during intestinal IRI. However, the organs through which Drp1 and NLRP3 regulate KC-mediated inflammatory response in IRI in hepatic steatosis have not been studied.

In this study, we verified the role of Kupffer cells in IRI in hepatic steatosis by *in vivo* and *in vitro* experiments. We found that after IRI in hepatic steatosis, Kupffer cells exacerbated the immune inflammatory response and IRI by promoting expression of NLRP3 and Drp1. Targeted inhibition of Drp1 not only reduced NLRP3 expression but also attenuated IRI in hepatic steatosis. The findings indicate that Kupffer-cell mediated immune inflammation is an important cause of exacerbating IRI in hepatic steatosis, and support Drp1 as a target for reducing IRI in hepatic steatosis, providing a potential solution for donor shortage and contributing to the prognosis of recipients with terminal-stage hepatic disease.

Methods

Animal and induction of hepatic steatosis

Male C57BL/6J specific-pathogen free mice 3–4 weeks of age were provided by the Experimental Animal Center of Drum Tower Hospital Affiliated to Nanjing University School of Medicine. The mice were housed at a constant temperature (21–23°C) in a 12-h day and night cycle with free access to drinking water. The mouse model of hepatic steatosis received high-fat diet (D12492; Research Diets, New Brunswick, NJ, USA) for 16–18 weeks. The control mice were fed a normal diet. The study was conducted following animal use and feeding standards established by the Committee of the China Animal Protection Association. The animal procedures were approved by the Institutional Animal Care and Use Committee of Nanjing University, Nanjing, China (No. 20180701).

Mouse hepatic ischemia-reperfusion model

The hepatic IRI model was prepared as previously described with slight modification.¹³ After inhaling isoflurane, the mice were placed in the supine position on the animal platform. The stomach and duodenum were pulled downward, and the left lobe of the liver was pushed upward to expose the hepatic hilum. The blood vessels supplying the left and middle lobes of the liver were clipped with a microscopic hemostatic clip to achieve partial liver ischemia. The clamping time was 0 min in the sham operation group and 60 min in the experimental IRI group. The microscopic hemostatic clip was opened to recanalize the hilar vessels. Mice were sacrificed 6 h after reperfusion, and blood and liver tissues were preserved. Total cholesterol (TC), triglycerides (TG), alanine aminotransferase (ALT), and aspartate aminotransferase (AST) levels in serum were determined by an automatic biochemical ana-

lyzer (NX700i; Fuji, Tokyo, Japan).

Histology and immunohistochemical (IHC) staining

To assess the degree of liver dysfunction, paraffin-embedded hepatic tissues were stained with hematoxylin and eosin (H&E). Liver injury was assessed by criteria described by Suzuki *et al.*¹⁴ During IHC staining, paraffin-embedded tissues were incubated with antibodies against F4/80+ (1:1,000, 29414-1-AP; Proteintech, Wuhan, China), NLRP3 (rabbit, 1:500, 27458-1-AP; Proteintech, Wuhan, China), and Drp1 (rabbit, 1:1,000, ab184247; Abcam).

Cell culture and H/R model

AML12 normal mouse liver cells and RAW264.7 mononuclear macrophage cells were purchased from the American Type Culture Collection (Manassas, VA, USA). AML12 cells were grown in DMEM containing 10% fetal bovine serum. RAW264.7 cells were grown in 1640 medium containing 10% fetal bovine serum. To assess H/R injury in cells, they were treated with hypoxic gas mixture (5% CO₂, 94% N₂, and 1% O₂) without fetal bovine serum and incubated at 37°C for 12 h. Subsequently, the cells were cultured for 4 h as previously described.¹⁵

Western blotting

Western blotting was conducted as previously described,¹⁶ which involved incubation with anti-NLRP3 (rabbit, 1:1,000, ab263899; Abcam), anti-Drp1 (rabbit, 1:1,000, ab184247; Abcam), and anti-actin (rabbit, 1:3,000, 20536-1-AP; Proteintech, Rosemont, IL, USA) antibodies. An Odyssey fluorescence scanner (Li-Cor Biosciences, Lincoln, NE, USA) was used to detect the signal from fluorescein-conjugated secondary antibodies. Image J (USA National Institutes of Health, Bethesda, MD, USA) software was used to measure and compare gray values.

Cell viability assay

AML12 and RAW264.7 cell suspensions were seeded in a 96-well plate at a density of 2×10⁵ cells per well before adding 100 μ L medium containing palmitate:oleic acid (1:2) at final concentrations of 100, 200, 300, 400, 500, 600, 800, and 1,000 μ M to each well and incubating for 48 h. Cell viability was determined with a cell counting kit-8 assay (TransGen, Beijing, China).

Real-time quantitative polymerase chain reaction (RT-qPCR)

The total RNA was extracted from AML-12 and RAW264.7 cells using Trizol reagent. Complementary DNA (cDNA) was synthesized with HiScript II RT SuperMix for qPCR+gDNA wiper (Yeasen Biotech, Shanghai, China), followed by RT-qPCR with SYBR Premix ExTaq (Yeasen Biotech) and detection using the ABI7500 real-time PCR system (Applied Biosystems, Foster City, CA, USA). The primers were Actin forward CTTCCCTCAGCACCTTCCAG and Actin reverse GCATCTCTGGTCCAGTAGGAA, NLRP3 forward AGGCTGCTATCTGGAGGAACT and NLRP3 reverse TTGCAACGGACTCGTCAT, Drp1 forward: GGCAGATATGCTGAAGGCAC and Drp1 reverse: AGCTGCCGTGACAGAAAACA.

Measurement of cytokine levels

Serum and supernatant levels of tumor necrosis factor alpha (TNF- α), interleukin (IL)-6, IL10, and IL1 β were determined by ELISA following the kit manufacturer's instructions (Solarbio, Beijing, China).

Statistical analysis

The results were reported as means±standard deviation (SD) and analyzed by PRISM 8 (<https://www.graphpad.com/features>). Multiple-group comparisons were performed by one-way analysis of variance, and $p < 0.05$, $p < 0.01$, and $p < 0.001$ were levels of significance.

Results

IRI was more serious in mice with fatty liver than it was in control mice

Male C57BL/6J mice at 3–4 weeks of age were fed a high-fat diet (Fig. 1A–F). The IRI model was established by 60 m of ischemia and 6 h of reperfusion and the sham group on underwent only exploratory laparotomy. The levels of ALT and AST in the IRI group were significantly higher than those in the Sham group (Fig. 1G, H), and the injured area of liver was significantly larger, with hepatic sinusoid stasis, hepatocyte swelling, and even hepatocyte necrosis (Fig. 1I and Supplementary Fig. 1A). Liver injury was studied after IRI in mice with fatty liver. The liver IRI model was established by the same protocol as described before. The results indicated that the ALT and AST levels in mice in HFD IRI group were significantly higher than those in the CD IRI group (Fig. 1J, K). The area of liver injury was significantly larger, and sinusoidal stasis, hepatocyte swelling, and hepatocyte necrosis were more severe (Fig. 1L and Supplementary Fig. 1B). The poor tolerance of IRI in hepatic steatosis may be an important restriction factor for becoming a marginal donor.

KCs aggravate IRI in hepatic steatosis

To explore the recruitment of KCs in the livers of CD mice after IRI, cells with F4/80 markers, a unique marker of murine macrophages, were detected by IHC staining of liver tissue. After liver ischemia-reperfusion in CD mice, the recruitment of F4/80+ cells in the necrotic area increased significantly (Fig. 2A). Further, we observed that the distribution of F4/80+ cells in the HFD IRI group was slightly different from that of the CD IRI group. In the HFD IRI group, F4/80+ cells were distributed diffusely in the liver tissue because of the more extensive area of hepatocytic necrosis (Fig. 2B). We explored the effect of eliminating KCs from IRI in hepatic steatosis. The hepatic IRI model was established in mice fed the HFD at the same week of age, as per the 60 m and 6 h IRI regimen. Three days before the operation, the experimental group (HFD CLO IRI group) was intraperitoneally injected with 400 μ L clodronate liposomes (CLO) and the control group (HFD IRI group) was intraperitoneally injected with 400 μ L dimethyl sulfoxide (DMSO). The results revealed that serum ALT and AST levels in the HFD CLO IRI group were significantly lower than those in the HFD IRI group (Supplementary Fig. 2A, B). HE staining revealed that hepatic sinusoid congestion and hepatocyte necrosis of mice in the HFD CLO IRI group were significantly less than those in the HFD IRI group (Fig. 2C). IHC staining confirmed the effective elimination of KCs in the liver by liposomal CLO (Fig. 2D). KCs are important immune cells in the liver, and their immune effects are enhanced in fatty livers, which aggravates the IRI.

Expression of NLRP3 and Drp1 decreased after IRI in normal livers

The levels of NLRP3 and Drp1 in the CD IRI group were considerably lower than those in the Sham group (Fig. 2E, H–J and Supplementary Fig. 3A). IHC staining confirmed these results (Fig. 2H–J). Further, we investigated the effect of hy-

poxia/reoxygenation on NLRP3 and Drp1 expression in non-steatotic cells *in vitro*. The results revealed that the protein and mRNA levels of NLRP3 and Drp1 were considerably decreased in AML12 and RAW264.7 cells (Fig. 2F, G, K–L, and Supplementary Fig. 3B, C). Therefore, NLRP3 and Drp1 were not up-regulated during the IRI in normal liver.

Expression of NLRP3 and Drp1 and inflammatory cytokines increased after IRI in hepatic steatosis

The levels of NLRP3 and Drp1 after IRI in hepatic steatosis were assessed *in vivo*. Western blot and IHC staining revealed that expression of NLRP3 and Drp1 in the HFD IRI group was significantly increased compared with the CD IRI group (Fig. 3A–C). Serum IL1 β , IL10, IL6, and TNF- α levels were significantly higher in the HFD IRI group than in the CD IRI group (Fig. 3D–G). Before constructing the steatosis cell model, CCK-8 assays were performed to determine the IC_{50s} of fatty acids in AML12 and RAW264.7 cells. A concentration of 300 μ M was selected for fatty acids (palmitic acid: oleic acid; 1:2), added to the culture medium, and incubated for 24 h. Oil red staining was used to verify the steatosis cell model (Fig. 3H–J). The results showed that the protein and mRNA levels of NLRP3 were slightly up-regulated ($p > 0.05$) in the steatosis group (FA H/R group) compared with the normal group (H/R group), but the expression of Drp1 was significantly decreased in mouse AML12 hepatocyte cells after 12 h of hypoxia and 6 h of reoxygenation preculture. In mouse macrophage RAW264.7 cells, the expression of the two proteins and mRNAs in the FA H/R group were significantly higher than those in H/R group (Fig. 3K, L and Supplementary Fig. 4A, B). The supernatant levels of IL1 β , IL10, IL6, and TNF- α in AML12 cells were significantly higher in the HFD IRI group compared with the CD IRI group (Fig. 3M). The results indicate that macrophages promoted NLRP3 and Drp1 immune activation and may aggravate IRI in hepatic steatosis.

Elimination of KCs reduced NLRP3 and Drp1 expression after IRI in hepatic steatosis

The effect of intrahepatic KCs on the levels of NLRP3 and Drp1 after IRI in hepatic steatosis was verified by western blotting and IHC staining. After IRI, compared with the HFD IRI group, the expression of NLRP3 and Drp1 in the livers of the HFD CLO IRI group were significantly decreased (Fig. 4A, C). Compared with the control group, the levels of NLRP3 and Drp1 in the livers of HFD mice lacking KCs decreased after IRI. Therefore, KCs, as innate immune cells of the liver, aggravated IRI in hepatic steatosis through NLRP3 and Drp1.

Inhibition of Drp1 decreased IRI, down-regulated the expression of NLRP3, and decreased the levels of inflammatory cytokines in hepatic steatosis

To explore the effect of Drp1 in IRI in mice fed an HFD, the mice in the HFD mdivi-1 IRI and HFD IRI groups were intraperitoneally injected with Drp1 inhibitor mdivi-1 (50 mg/kg) and normal saline 2 h before the operation. ALT and AST levels in the HFD mdivi-1 IRI group were considerably lower than those in the HFD IRI group (Supplementary Fig. 5A, B). HE staining revealed that the liver injury area, sinus congestion, and hepatocytic necrosis in mice in the HFD mdivi-1 IRI group were significantly decreased compared with those in the HFD IRI group (Fig. 4D). Western blotting revealed that the protein levels of NLRP3 and Drp1 in the HFD mdivi-1 group were decreased (Fig. 4B). IHC staining of mouse liver tissue revealed the same results (Fig. 4E). Compared with the HFD IRI group, the serum IL1 β , IL10, IL6, and TNF- α

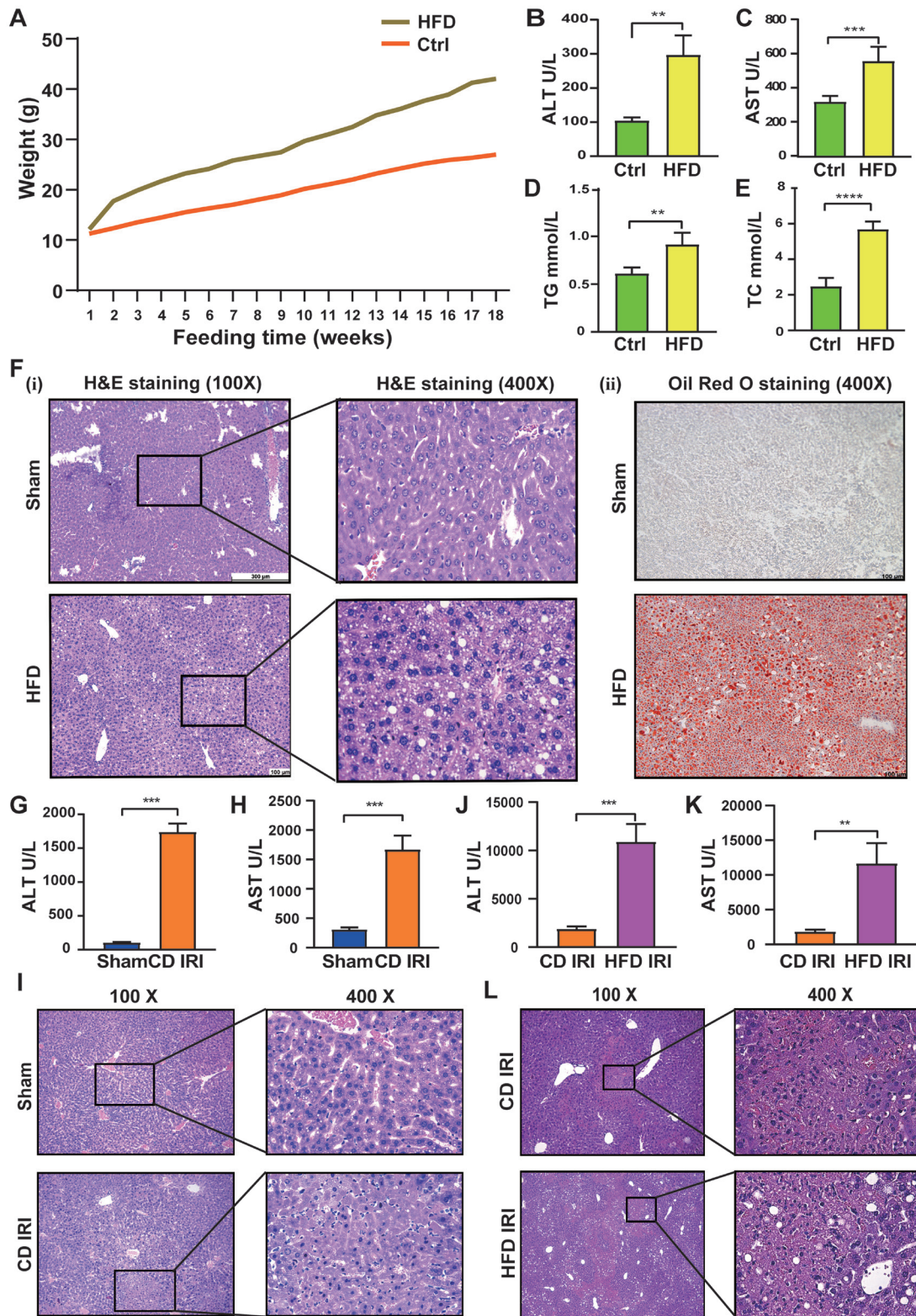


Fig. 1. Ischemia-reperfusion injury was significantly increased in mice with fatty livers. (A) Changes in body weight between HFD and Ctrl groups. (B–E) Serum TC, TG, ALT, AST contents of mice after 16 weeks of HFD and Ctrl groups 4 ($n=5-7$ mice per group). (F) HE staining and oil red staining of liver of mice on HFD and Ctrl groups. (G, H) Serum levels of ALT and AST in the CD IRI and sham groups ($n=5-7$ mice per group); (J, K) Serum levels of ALT and AST in HFD IRI group and CD IRI group ($n=5-7$ mice per group); (I) HE staining of liver in CD IRI and Sham groups; (L) HE staining of liver in the HFD IRI and CD IRI groups. HFD, high-fat diet; Ctrl, ordinary diet; Sham, sham operation group; CD IRI, normal diet ischemia-reperfusion group; HFD IRI, high-fat diet ischemia-reperfusion group; H&E, hematoxylin and eosin.

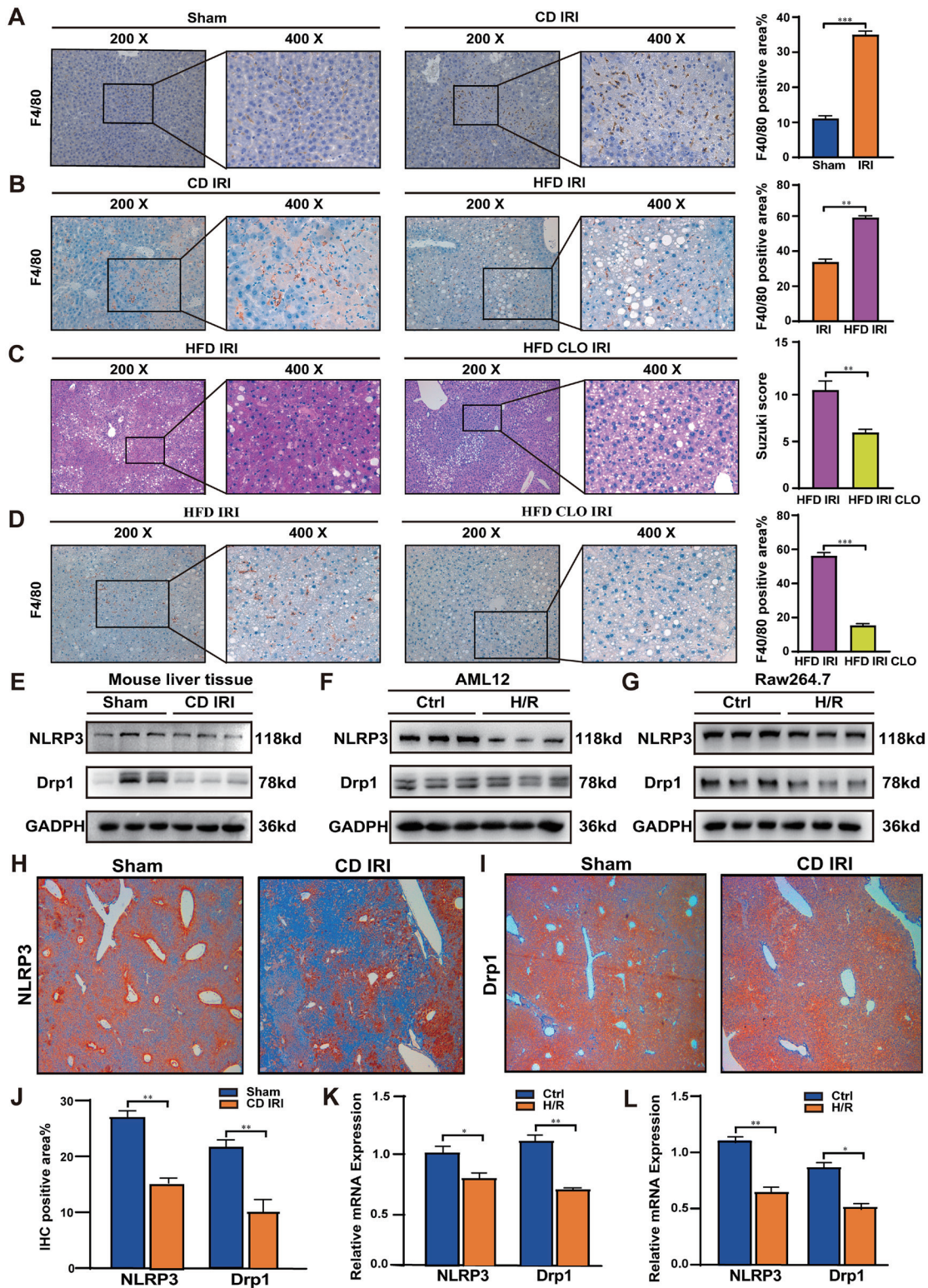


Fig. 2. Kupffer cells aggravate ischemia-reperfusion injury in hepatic steatosis. (A) F4/80 cells were detected by IHC of liver tissue in CD IRI group and Sham group. (B) F4/80 cells were detected by IHC of liver tissue in HFD IRI group and CD IRI group. (C) HE staining of liver in HFD CLO IRI group and HFD IRI group; (D) F4/80 cells were detected by in HFD CLO IRI group and HFD IRI group; (E) the protein expression of NLRP3 and Drp1 in the liver of Sham and CD IRI groups. (F and G) the protein expression of NLRP3 and Drp1 in the AML12 and RAW264.7 of Ctrl and H/R groups. (H–J) NLRP3 and Drp1 were detected by IHC of liver tissue in Sham and CD IRI groups. (K and L) the mRNA expression of NLRP3 and Drp1 in the AML12 and RAW264.7 of Ctrl and H/R groups using RT-qPCR. Drp1, dynamics-associated protein 1; IHC, immunohistochemistry; NLRP3, NOD-like receptor thermal protein domain-associated protein 3; RT-qPCR, real-time quantitative polymerase chain reaction.

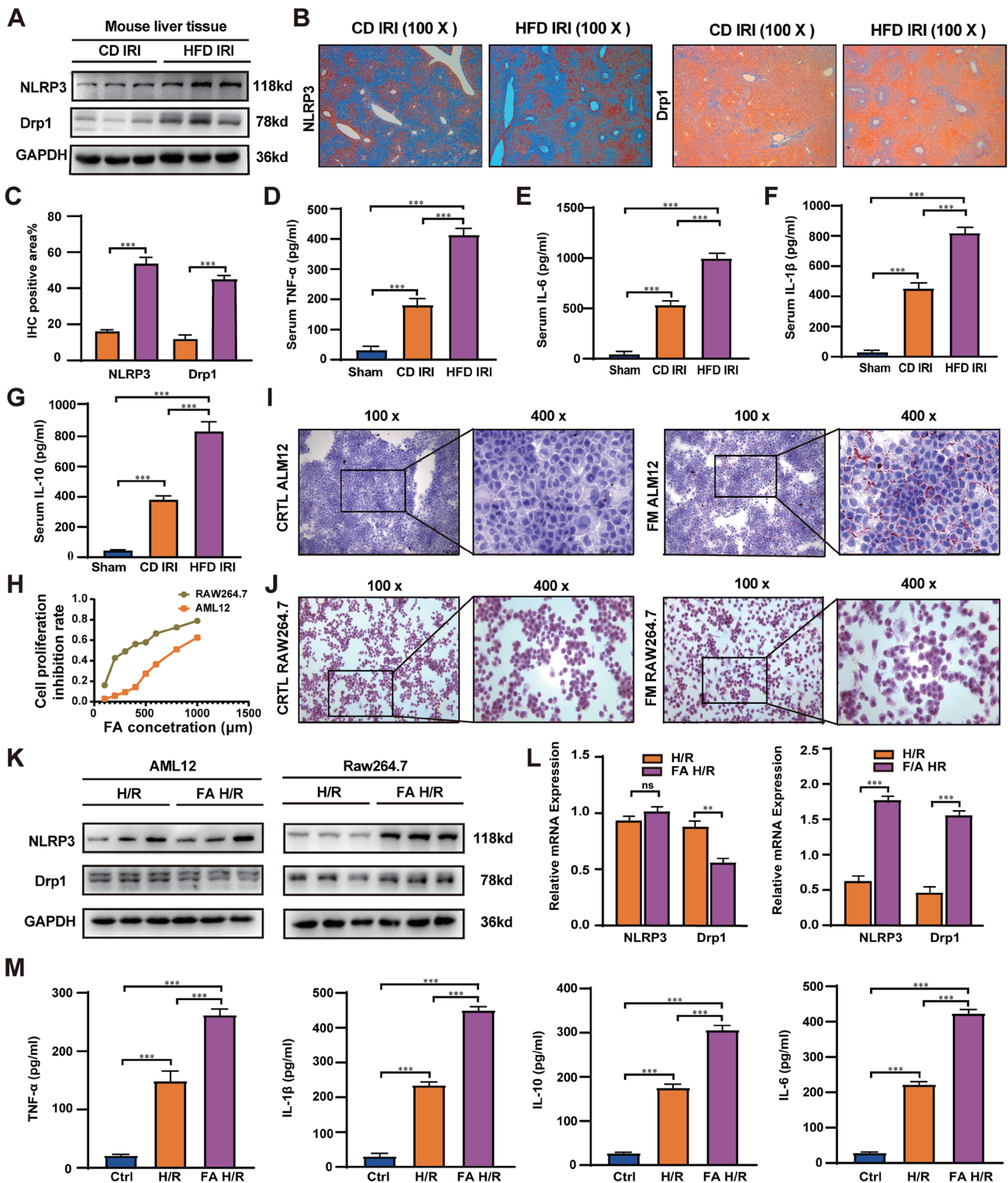


Fig. 3. Kupffer cells aggravate ischemia-reperfusion injury in hepatic steatosis by upregulating Drp1 and NLRP3. (A–C) NLRP3 and Drp1 expression in liver tissue from the HFD IRI and CD IRI groups assayed by western blotting and IHC. (D–G) Serum IL1 β , IL10, IL6, and TNF- α assayed after sham treatment and in the CD IRI and HFD IRI groups ($n=5-6$ mice per group). (H) Inhibition of the proliferation of AML12 and RAW264.7 cells by fatty acids. (K, J) HE and Oil red staining was used to detect intracellular lipid droplets to verify the success of the model of cellular steatosis. (F, E) Protein and mRNA expression of NLRP3 and Drp1 in the AML12 and RAW264.7 of HFD IRI and CD IRI groups using Western Blotting and RT-qPCR. (F) supernatant IL1 β , IL10, IL6, and TNF- α was assayed in the Ctrl, H/R and FA H/R groups by ELISA. Ctrl, Control group; Drp1, dynamics-associated protein 1; ELISA, enzyme-linked immunosorbent assay; FA, fatty acid culture group; H&E, hematoxylin and eosin; IHC, immunohistochemistry; NLRP3, NOD-like receptor thermal protein domain-associated protein 3; RT-qPCR, real-time quantitative polymerase chain reaction.

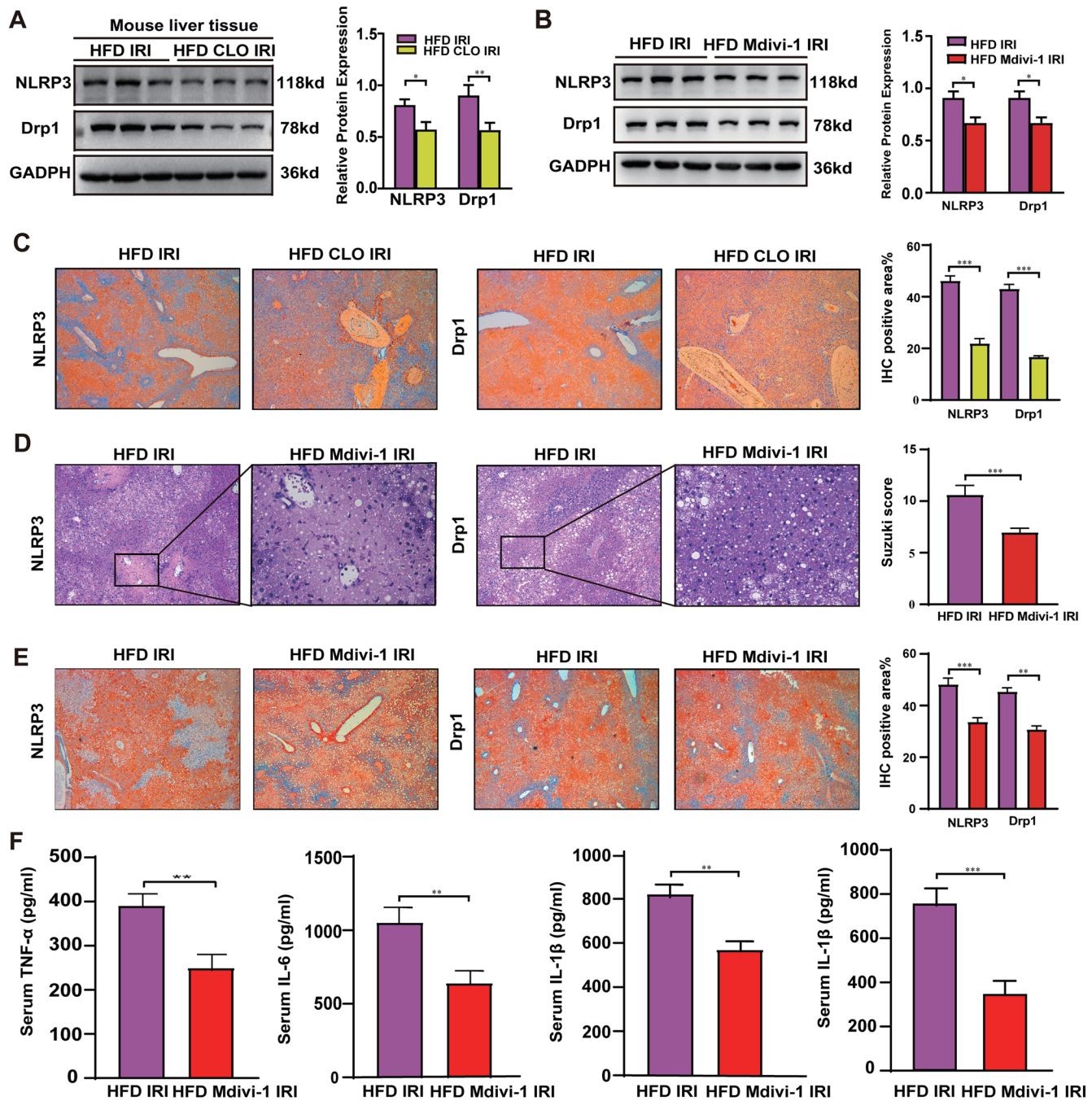


Fig. 4. Inhibition of Drp1 down-regulated NLRP3 expression and reduce IRI in hepatic steatosis. (A and C) Expression of NLRP3 and Drp1 in the liver of HFD CLO IRI and HFD IRI groups. (B and E) NLRP3 and Drp1 expression in the liver tissue from the HFD Mdivi-1 IRI and HFD IRI groups using IHC and Western Blotting (D) HE staining of liver in the HFD Mdivi-1 IRI and HFD IRI groups. (F) Serum IL-1 β , IL-10, IL-6, and TNF- α was measured assayed in the HFD Mdivi-1 IRI and HFD IRI groups by ELISA. ELISA, enzyme-linked immunosorbent assay; H&E, hematoxylin and eosin; IHC, immunohistochemistry.

levels were significantly decreased in the HFD mdivi-1 IRI group (Fig. 4F). Therefore, inhibition of Drp1, which attenuated NLRP3 expression and IRI in fatty liver, and can be a specific therapeutic strategy.

Discussion

For patients with terminal-stage hepatic disease, liver trans-

plantation is a promising treatment. However, the number of patients waiting for liver transplantation is increasing year by year, and the shortage of liver donors has become a serious problem.¹⁷ Donors with fatty livers are widely accepted by medical centers as marginal liver donors to solve the problem of donor shortage.¹⁸ Donors with steatosis are particularly vulnerable to IRI, and the incidence of graft nonfunction is high after transplantation.² Compared with mice fed on a

regular diet, graft dysfunction was detected when the liver from mice donors with fatty liver was used.¹⁹ It is generally believed that livers with steatosis are more susceptible to IRI than the normal liver. Multiple factors and pathways aggravate IRI in fatty liver. Zhang *et al.*²⁰ reported that TLR4 increased the levels of TNF- α and IL-6, inhibited levels of PGC-1 α and Mfn2, reduced mitochondrial fusion in IRI in NAFLD, and significantly aggravated IRI. Nii *et al.*²¹ reported that hydrolyzed whey peptide had an anti-inflammatory role and alleviated liver injury by reducing the levels of TNF- α , IL6, iNOS, and uncoupling protein-2 (UCP2) in the liver of NAFLD rats with IRI. Our results revealed that IRI in fatty liver was more significant than that in livers with no steatosis. The serum levels of ALT and AST were significantly increased, and the area of liver injury was significantly expanded. That was manifested as hepatic sinusoidal stasis and hepatocytic swelling and necrosis. More attention should be paid to the prevention and treatment of IRI when the liver from a marginal donor is used as a graft.

IRI is a type of aseptic inflammatory injury in which the activation of the innate immune system has an important role. KCs in the hepatic sinusoids are integral to the immune response.^{22,23} Some studies have reported that hepatic ischemia-reperfusion increased the infiltrating M1-state macrophages in the liver lobe.²⁴ Wei *et al.*²⁵ reported that ischemia led to increase of anaerobic glycolysis and lactic acid accumulation, formation of acidic microenvironment, inhibition of PPAR- γ , and transformation of macrophages to M1 state, further aggravating IRI. Naroa *et al.*²⁶ reported that knockdown of endogenous negative regulator of methylation-controlled J protein (MCJ) restored the mitochondrial energy supply, regulated immune responses, accelerated the initiation and process of liver regeneration through G1/S phase conversion, and prevented cell death after IRI. Therefore, macrophage activation is an important part of ischemia-reperfusion in the liver.

This study demonstrated that KCs were activated during hepatic IRI and were recruited in the necrotic area. The IRI in hepatic steatosis was more severe, and the activation of KCs was greater, which is diffusely distributed in various necrotic areas in the liver. The elimination of macrophages in fatty liver significantly reduced IRI in fatty livers. The study results confirmed that KCs aggravated IRI in the liver.

The results of *in vitro* and *in vivo* experiments demonstrated that IRI in hepatic steatosis increased the secretion of inflammatory factors, and serum inflammatory factor levels were significantly reduced by targeted inhibition of Drp1. TNF- α and IL1 β are two of the most important cytokines that aggravate liver IRI.²⁷ KCs are the main site of IL1 β production, and IL1 β production mainly occurs through the activation of NLR inflammasomes. In addition, activation of NLRP3 in hepatic macrophages releases TNF- α ; thus, the activation of NLRP3 in KCs is an important link in IRI in hepatic steatosis. NLRP3 is an intracellular sensor that is mostly inactive and ubiquitinated in the stable state.²⁸ Various upstream signals induce intracellular formation and activation of NLRP3 inflammasome through two different modes: PAMPs and DAMPs. Subsequently, caspase-1 is cleaved and activated to mediate tissue inflammation.²⁹ Inflammatory factors are linked to IRI in hepatic steatosis. Reducing inflammatory responses is a promising strategy to alleviate IRI in hepatic steatosis.

Oxidative stress is high in hepatic steatosis, and its level is related to the severity of nonalcoholic fatty liver disease (NAFLD).³⁰ After liver ischemia-reperfusion, a cascade causing oxidative stress is activated; however, the antioxidant system is inhibited. The clearance of reactive oxygen species

(ROS) is reduced, leading to a sharp increase in ROS, which produces oxidized protein that acts as a ligand for NLRP3 activation.³¹ Similar findings were reported in this study. Mice with fatty livers produced more ROS because of the presence of fatty acids and oxidative stress. ROS production was increased after ischemia-reperfusion, significantly increasing the expression of NLRP3 and aggravating tissue damage. After hypoxia and reoxygenation, NLRP3 expression was only slightly increased *in vitro* in hepatocytes with steatosis compared with those with no steatosis, but was significantly increased in macrophages with steatosis. The results suggest that the increase of NLRP3 expression in fatty liver with IRI was mediated by KCs.

IRI involves oxidative stress response, inflammation, Ca²⁺ overload, and apoptosis, and these pathological processes are closely associated with mitochondrial dysfunction.³² Mitochondrial dynamics regulate the structure and function of mitochondria, which is manifested as the fusion and fission of mitochondria. Drp1 is one of the major proteins regulating mitochondrial fission. Drp1 is dispersed in the cytoplasm and is recruited from the cytoplasm to break sites on the mitochondrial surface after mitochondrial fission is activated.³³ Archer *et al.*³⁴ found that Drp1 inhibitors protected cardiomyocytes from IRI by reducing ROS production and maintaining mitochondrial dynamics. Qasim *et al.*³⁵ reported that during intestinal ischemia-reperfusion, translocation of Drp1 to the outer mitochondrial membrane was inhibited, thus inhibiting mitochondrial fission and ROS generation to improve cell damage during intestinal ischemia-reperfusion. The above studies indicated that Drp1 cleaved mitochondria and promoted ROS production.

The production of ROS activates NLRP3 inflammasomes, and Drp1 promotes the activation of NLRP3 inflammasomes. Several studies have reported that Drp1 activation promoted NLRP3 activation, leading to aggravation of tissue damage or disease progression in various diseases. However, inhibition of Drp1 activation has beneficial effects.³⁶ Zhang *et al.*³⁷ reported that overactivation of Drp1 in mature oligodendrocytes triggered NLRP3-related inflammation by inhibiting hexokinase 1, which may be a key mechanism in Alzheimer's disease. Some studies reported that down-regulation of Drp1 expression or knockdown of *Drp1* gene reduced the production of ROS and contributed to the inhibition of NLRP3, caspase-1, IL- β protein expression, and cancer cell migration.³⁸ In this study, the use of mdivi-1, a Drp1 inhibitor, reduced the expression of NLRP3 in fatty liver with IRI and in turn reduced the severity of injury. Drp1 may be used as a target to protect fatty liver from IRI.

This study demonstrated that activation of KCs aggravated IRI in hepatic steatosis. The mechanism may involve KC-mediated inflammatory responses that stimulated the formation of NLRP3 inflammasomes that activated Drp1. It caused the dysfunction of mitochondrial dynamics and aggravated IRI in hepatic steatosis. Drp1 inhibitors effectively attenuated KC-mediated immune inflammatory responses and protected against the deleterious consequences of ischemia-reperfusion in hepatic steatosis. More *in vivo* experiments are needed to verify the effect of KCs on IRI in fatty liver using macrophage-deficient mice; the experimental results may be better verified in the hepatic IRI after macrophage infusion.

Conclusions

This study verified that fatty liver reduced the tolerance of liver tissue to ischemia and hypoxia, and IRI was more severe than that in the normal liver. In terms of mechanism,

fatty liver promoted the stimulation of KCs in the liver and increased the expression of Drp1. Subsequently, the expression of NLRP3 was increased, aggravating IRI in hepatic steatosis. mdivi-1, a Drp1 inhibitor, reduced the expression of NLRP3 and alleviated IRI of fatty livers. The study provides new insights for the prevention of IRI in hepatic steatosis.

Funding

None to declare.

Conflict of interest

The authors have no conflict of interests related to this publication.

Author contributions

Conceived and designed the study (MW, MC, HD), collected and assembled the data (LZ, RA, JD, SL, MW, CM, HD), performed the data analysis and interpretation (LZ, RA, JD, SL), wrote the manuscript (LZ, RA, JD), and provided financial support and gave final approval of the manuscript (MW, MC, HD). All authors read and approved the manuscript.

Ethical statement

The animal procedures were approved by the Institutional Animal Care and Use Committee of Nanjing University, Nanjing, China (No. 20180701).

Data sharing statement

No additional data are available.

References

[1] Goldaracena N, Cullen JM, Kim DS, Eksler B, Halazun KJ. Expanding the donor pool for liver transplantation with marginal donors. *Int J Surg* 2020;82S:30–35. doi:10.1016/j.ijss.2020.05.024, PMID:32422385.

[2] Elias-Miro M, Mendes-Braz M, Cereijo R, Villarroya F, Jimenez-Castro MB, Gracia-Sancho J, *et al*. Resistin and visfatin in steatotic and non-steatotic livers in the setting of partial hepatectomy under ischemia-reperfusion. *J Hepatol* 2014;60(1):87–95. doi:10.1016/j.jhep.2013.07.041, PMID:23968888.

[3] van der Heide D, Weiskirchen R, Bansal R. Therapeutic Targeting of Hepatic Macrophages for the Treatment of Liver Diseases. *Front Immunol* 2019;10:2852. doi:10.3389/fimmu.2019.02852, PMID:31849997.

[4] Xu H, Li H, Woo SL, Kim SM, Shende VR, Neuendorff N, *et al*. Myeloid cell-specific disruption of Period1 and Period2 exacerbates diet-induced inflammation and insulin resistance. *J Biol Chem* 2014;289(23):16374–16388. doi:10.1074/jbc.M113.539601, PMID:24770415.

[5] Cai Y, Li H, Liu M, Pei Y, Zheng J, Zhou J, *et al*. Disruption of adenosine 2A receptor exacerbates NAFLD through increasing inflammatory responses and SREBP1c activity. *Hepatology* 2018;68(1):48–61. doi:10.1002/hep.29777, PMID:29315766.

[6] Musso G, Cassader M, Gambino R. Non-alcoholic steatohepatitis: emerging molecular targets and therapeutic strategies. *Nat Rev Drug Discov* 2016;15(4):249–274. doi:10.1038/nrd.2015.3, PMID:26794269.

[7] Rathinam VA, Fitzgerald KA. Inflammasome Complexes: Emerging Mechanisms and Effector Functions. *Cell* 2016;165(4):792–800. doi:10.1016/j.cell.2016.03.046, PMID:27153493.

[8] Cai C, Zhu X, Li P, Li J, Gong J, Shen W, *et al*. NLRP3 Deletion Inhibits the Non-alcoholic Steatohepatitis Development and Inflammation in Kupffer Cells Induced by Palmitic Acid. *Inflammation* 2017;40(6):1875–1883. doi:10.1007/s10753-017-0628-z, PMID:28730512.

[9] Ma E, Xing H, Pei J, Zhang Q, Li R, Shen C, *et al*. Itaconic acid facilitates inflammation abatement and alleviates liver ischemia-reperfusion injury by inhibiting NF-kappaB/NLRP3/caspase-1 inflammasome axis. *Ann Transl Med* 2022;10(16):861. doi:10.21037/atm-22-3388, PMID:36111043.

[10] Fuertes-Agudo M, Luque-Tevar M, Cucarella C, Brea R, Bosca L, Quintana-Cabrera R, *et al*. COX-2 Expression in Hepatocytes Improves Mitochondrial Function after Hepatic Ischemia-Reperfusion Injury. *Antioxidants* (Basel) 2022;11(9):1724. doi:10.3390/antiox11091724, PMID:36139798.

[11] Anand R, Langer T, Baker MJ. Proteolytic control of mitochondrial function and morphogenesis. *Biochim Biophys Acta* 2013;1833(1):195–204.

doi:10.1016/j.bbamcr.2012.06.025, PMID:22749882.

[12] Qasim W, Li Y, Tian XF. PTEN-induced kinase 1-induced dynamin-related protein 1 Ser637 phosphorylation reduces mitochondrial fission and protects against intestinal ischemia reperfusion injury. *World J Gastroenterol* 2020;26(15):1758–1774. doi:10.3748/wjg.v26.i15.1758, PMID:32351292.

[13] Shang L, Ren H, Wang S, Liu H, Hu A, Gou P, *et al*. SS-31 Protects Liver from Ischemia-Reperfusion Injury via Modulating Macrophage Polarization. *Oxid Med Cell Longev* 2021;2021:6662156. doi:10.1155/2021/6662156, PMID:33986918.

[14] Suzuki S, Toledo-Pereyra LH, Rodriguez FJ. Neutrophil infiltration as an important factor in liver ischemia and reperfusion injury. Modulating effects of FK506 and cyclosporine. *Transplantation* 1993;55(6):1265–1272. doi:10.1097/00007890-199306000-00011, PMID:7685932.

[15] Ming N, Na HST, He JL, Meng QT, Xia ZY. Propofol alleviates oxidative stress via upregulating lncRNA-TUG1/Brg1 pathway in hypoxia/reoxygenation hepatic cells. *J Biochem* 2019;166(5):415–421. doi:10.1093/jb/mvz054, PMID:31297532.

[16] Hao S, Ji J, Zhao H, Shang L, Wu J, Li H, *et al*. Mitochondrion-Targeted Peptide SS-31 Inhibited Oxidized Low-Density Lipoproteins-Induced Foam Cell Formation through both ROS Scavenging and Inhibition of Cholesterol Influx in RAW264.7 Cells. *Molecules* 2015;20(12):21287–21297. doi:10.3390/molecules201219764, PMID:2663327.

[17] Metin O, Simsek C, Gurakar A. Update on liver transplantation-newer aspects. *Turk J Med Sci* 2020;50(S1-2):1642–1650. doi:10.3906/sag-2002-17, PMID:32222125.

[18] Jimenez-Castro MB, Casillas-Ramirez A, Negrete-Sanchez E, Avalos-de Leon CG, Gracia-Sancho J, Peralta C. Adipocytokines in Steatotic Liver Surgery/Transplantation. *Transplantation* 2019;103(1):71–77. doi:10.1097/TP.0000000000002098, PMID:30586349.

[19] Chu MJ, Dare AJ, Phillips AR, Bartlett AS. Donor Hepatic Steatosis and Outcome After Liver Transplantation: a Systematic Review. *J Gastrointest Surg* 2015;19(9):1713–1724. doi:10.1007/s11605-015-2832-1, PMID:25917535.

[20] Zhang C, Jia Y, Liu B, Wang G, Zhang Y. TLR4 knockout upregulates the expression of Mfn2 and PGC-1alpha in a high-fat diet and ischemia-reperfusion mice model of liver injury. *Life Sci* 2020;254:117762. doi:10.1016/j.lfs.2020.117762, PMID:32437795.

[21] Nii A, Utsunomiya T, Shimada M, Ikegami T, Ishibashi H, Imura S, *et al*. Hydrolyzed whey peptide-based diet ameliorates hepatic ischemia-reperfusion injury in the rat nonalcoholic fatty liver. *Surg Today* 2014;44(12):2354–2360. doi:10.1007/s00595-014-0853-0, PMID:24492979.

[22] Ikarashi M, Nakashima H, Kinoshita M, Sato A, Nakashima M, Miyazaki H, *et al*. Distinct development and functions of resident and recruited liver Kupffer cells/macrophages. *J Leukoc Biol* 2013;94(6):1325–1336. doi:10.1189/jlb.0313144, PMID:23964119.

[23] Krenkel O, Tacke F. Liver macrophages in tissue homeostasis and disease. *Nat Rev Immunol* 2017;17(5):306–321. doi:10.1038/nri.2017.11, PMID:28317925.

[24] Yazdani HO, Kaltenmeier C, Morder K, Moon J, Traczek M, Loughran P, *et al*. Exercise Training Decreases Hepatic Injury and Metastases Through Changes in Immune Response to Liver Ischemia/Reperfusion in Mice. *Hepatology* 2021;73(6):2494–2509. doi:10.1002/hep.31552, PMID:32924145.

[25] Ding W, Duan Y, Qu Z, Feng J, Zhang R, Li X, *et al*. Acidic Microenvironment Aggravates the Severity of Hepatic Ischemia/Reperfusion Injury by Modulating M1-Polarization Through Regulating PPAR-gamma Signal. *Front Immunol* 2021;12:697362. doi:10.3389/fimmu.2021.697362, PMID:34234785.

[26] Goikoetxea-Usandizaga N, Serrano-Macia M, Delgado TC, Simon J, Fernandez Ramos D, Barriales D, *et al*. Mitochondrial bioenergetics boost macrophage activation, promoting liver regeneration in metabolically compromised animals. *Hepatology* 2022;75(3):550–566. doi:10.1002/hep.32149, PMID:34510498.

[27] Li P, He K, Li J, Liu Z, Gong J. The role of Kupffer cells in hepatic diseases. *Mol Immunol* 2017;85:222–229. doi:10.1016/j.molimm.2017.02.018, PMID:28314211.

[28] Qiao Y, Wang P, Qi J, Zhang L, Gao C. TLR-induced NF-kappaB activation regulates NLRP3 expression in murine macrophages. *FEBS Lett* 2012;586(7):1022–1026. doi:10.1016/j.febslet.2012.02.045, PMID:22569257.

[29] Jo EK, Kim JK, Shin DM, Sasakawa C. Molecular mechanisms regulating NLRP3 inflammasome activation. *Cell Mol Immunol* 2016;13(2):148–159. doi:10.1038/cmi.2015.95, PMID:26549800.

[30] Ni HY, Yu L, Zhao XL, Wang LT, Zhao CJ, Huang H, *et al*. Seed oil of Rosa roxburghii Tratt against non-alcoholic fatty liver disease in vivo and in vitro through PPARalpha/PGC-1alpha-mediated mitochondrial oxidative metabolism. *Phytomedicine* 2022;98:153919. doi:10.1016/j.phymed.2021.153919, PMID:35104757.

[31] Tang SP, Mao XL, Chen YH, Yan LL, Ye LP, Li SW. Reactive Oxygen Species Induce Fatty Liver and Ischemia-Reperfusion Injury by Promoting Inflammation and Cell Death. *Front Immunol* 2022;13:870239. doi:10.3389/fimmu.2022.870239, PMID:35572532.

[32] Tilokani L, Nagashima S, Paupe V, Prudent J. Mitochondrial dynamics: overview of molecular mechanisms. *Essays Biochem* 2018;62(3):341–360. doi:10.1042/EBC20170104, PMID:30030364.

[33] Huang J, Xie P, Dong Y, An W. Inhibition of Drp1 SUMOylation by ALR protects the liver from ischemia-reperfusion injury. *Cell Death Differ* 2021;28(4):1174–1192. doi:10.1038/s41418-020-00641-7, PMID:33110216.

[34] Wu D, Dasgupta A, Chen KH, Neuber-Hess M, Patel J, Hurst TE, *et al*. Identification of novel dynamin-related protein 1 (Drp1) GTPase inhibitors: Therapeutic potential of Drpitor1 and Drpitor1a in cancer and cardiac ischemia-reperfusion injury. *FASEB J* 2020;34(1):1447–1464. doi:10.1096/fj.201901467R, PMID:31914641.

- [35] Qasim W, Li Y, Sun RM, Feng DC, Wang ZY, Liu DS, *et al*. PTEN-induced kinase 1-induced dynamin-related protein 1 Ser637 phosphorylation reduces mitochondrial fission and protects against intestinal ischemia reperfusion injury. *World J Gastroenterol* 2020;26(15):1758–1774. doi:10.3748/wjg.v26.i15.1758, PMID:32351292.
- [36] Zeng C, Duan F, Hu J, Luo B, Huang B, Lou X, *et al*. NLRP3 inflammasome-mediated pyroptosis contributes to the pathogenesis of non-ischemic dilated cardiomyopathy. *Redox Biol* 2020;34:101523. doi:10.1016/j.redox.2020.101523, PMID:32273259.
- [37] Zhang X, Wang R, Qi X. Oligodendroglial glycolytic stress triggers inflammasome activation and neuropathology in Alzheimer's disease. *Sci Adv* 2020;6(49):eabb8680. doi:10.1126/sciadv.abb8680, PMID:33277246.
- [38] Si L, Fu J, Liu W, Hayashi T, Nie Y, Mizuno K, *et al*. Silibinin inhibits migration and invasion of breast cancer MDA-MB-231 cells through induction of mitochondrial fusion. *Mol Cell Biochem* 2020;463(1-2):189–201. doi:10.1007/s11010-019-03640-6, PMID:31612353.